Biochimica et Biophysica Acta 1860 (2016) 2086–2096

Contents lists available at ScienceDirect

Biochimica et Biophysica Acta

journal homepage: www.elsevier.com/locate/bbagen

Effect of DNA bending on transcriptional interference in the systems of closely spaced convergent promoters

Olga N. Koroleva [a,*], Evgeniy V. Dubrovin [a,b,*], Igor V. Yaminsky [a], Valeriy L. Drutsa [a]

[a] Lomonosov Moscow State University, Leninskie Gory, 1, Moscow 119991, Russian Federation
[b] Federal Research and Clinical Center of Physical-Chemical Medicine, Malaya Pirogovskaya, 1a, Moscow 119435, Russian Federation

ARTICLE INFO

Article history:
Received 2 March 2016
Received in revised form 27 June 2016
Accepted 29 June 2016
Available online 01 July 2016

Keywords:
Convergent transcription
Transcription interference
E. coli RNA polymerase
DNA structure
Open promoter complexes
Atomic force microscopy

ABSTRACT

Background: Over the past years there are increasing evidences that the interplay between two molecules of RNA polymerases, initiating transcription from promoters, oriented in opposite (convergent) directions, can serve as a regulatory factor of gene expression. The data concerning the molecular mechanisms of this so-called transcriptional interference (TI) are not well understood.
Methods: The interaction of RNA polymerase with circular DNA templates, containing the convergent promoters, was investigated in a series of *in vitro* transcription assays and atomic force microscopy (AFM).
Results: In this work, to study the mechanisms of transcription interference a series of plasmids with oppositely oriented closely spaced artificial promoters, recognized by *Escherichia coli* RNA polymerase, was constructed. The constructs differ in promoter structure and distance between the transcription start sites. We have demonstrated that the transcripts ratio (RNA-R/RNA-L) and morphology of convergent open promoter complexes (OPC) are highly dependent on the interpromoter distance.
Conclusions: The obtained results allowed us to suggest the novel model of TI, which assumes the DNA bending upon binding of RNA polymerase with promoters and explains the phenomenon of complete inactivation of weaker promoter by the stronger one.
General significance: The results show that the conformational transitions in DNA helix, associated with DNA bending upon binding of RNA polymerase with promoters, play crucial role in OPC formation in the systems with convergent promoters.

1. Introduction

Regulation of gene expression in bacteria occurs mainly at the level of transcription. Over the past years, increasing attention has been directed towards a special type of regulation, i.e. transcriptional interference, associated with interplay between two molecules of RNA polymerases (RNAP), initiating transcription from closely spaced promoters, oriented in the same (tandem) or opposite (convergent) directions. In the latter case the effect of transcription suppression is most pronounced [1–3]. The peculiarities of convergent transcription were investigated in a number of systems, including both naturally occurred and artificial ones [4–8]. The most common observation is significant suppression of transcription (up to complete inactivation) directed from "weaker" promoter in the presence of the second stronger opposite promoter [4,7,9]. Several mechanisms have been proposed to explain various effects observed. In particular, TI can be realized via several different possible pathways, i.e. the opposite promoter occlusion by transcribing RNAP molecule, collision of elongating RNAP molecule with the second one bound to opposite promoter ("sitting duck"), collision of two elongating RNAP molecules, RNA interference due to the sense-antisense interaction of partially complementary transcripts [1, 10–14]. The presence of collided complexes in some model systems was directly demonstrated by atomic force microscopy (AFM) [15]. However, the mechanisms of TI observed in any particular case, are still not clear. Various factors can affect the convergent transcription suppression: mutual orientation and distance between promoters, relative promoter strength, the structure of DNA template, etc. [7,13,14]. At present, the estimation of the role of these factors is problematic because it is difficult to compare correctly the data, obtained under variable conditions with the use of structurally different promoters. A special system of identical DNA templates with systematic variation of

* Corresponding authors at: Lomonosov Moscow State University, Leninskie Gory, 1, Moscow 119991, Russian Federation.
E-mail addresses: koroleva@genebee.msu.ru (O.N. Koroleva), dubrovin@polly.phys.msu.ru (E.V. Dubrovin).

http://dx.doi.org/10.1016/j.bbagen.2016.06.026
0304-4165/

structural elements of convergent promoters module (interpromoter distance and orientation, promoter sequences) would be very useful.

In this work, with the purpose to clarify the contribution of various structural factors to TI, a collection of plasmids with oppositely oriented artificial promoters recognized by *Escherichia coli* RNA polymerase, was constructed. The constructs differ in the structure of promoters and distance between transcription start sites. The interaction of RNA polymerase with convergent promoters was investigated in the *in vitro* systems of run-off transcription and AFM experiments. Direct AFM visualization of DNA molecules and DNA-protein complexes including transcriptional ones at a single molecule level allows their characterization and discrimination by topographical characteristics and mechanical properties [15–22]. The data obtained allowed us to suggest the novel mechanism of TI, which accounts for various above mentioned effects, including complete inactivation of weaker promoter by the convergent stronger one. This "narrow pocket" mechanism takes into consideration the role of physical structure of DNA template, in particular, the presence of bends within DNA double-helix arising from the interaction of RNAP with promoters. The effects observed are highly dependent on the interpromoter distance.

2. Materials and methods

Ribonucleoside triphosphates ATP, GTP, CTP, and UTP were purchased from Boehringer (Germany), heparin was from Sigma (USA), ampicillin was from Serva (Germany); tryptone, yeast extract and MacConkey agar were from Difco (USA). γ-^{32}P-ATP (185 PBq/mol) and α-^{32}P-UTP (148 PBq/mol) were from Isotope (Obninsk, Russia).

The enzymes T4 polynucleotide kinase, T4 DNA ligase, *Escherichia coli* DNA polymerase I, Klenow fragment of DNA polymerase, *Pfu* DNA polymerase and exonuclease III were purchased from Fermentas (Lithuania), *Escherichia coli* RNA polymerase holoenzyme (1.1 μg/μl, 1.2 activity units/μl) was from Epicentre Technology (USA), S1 nuclease (300 un./μl) was from Boehringer (Germany). The structures of all synthetic oligodeoxyribonucleotides (Sintol, Russia) used in this work are given in the Supplementary material (Table S1).

Polymerase chain reactions (PCR) were performed in a programmed CycloTemp-107 thermostat (Resurs-Pribor, Russia).

Electrophoresis of polynucleotides was performed in 8% denaturing polyacrylamide gel in glass plates (25 × 20 × 0.04 cm) in Tris-borate buffer (pH 8.3) containing 8 M urea at the field strength of 50 V/cm.

Escherichia coli cells DH5α (*lac*$^-$), ER1821, JM109 and JM110 were used as host strains during plasmid preparation. Transformation, cloning, isolation of the plasmid DNA, purification of DNA fragments in gels, and also other procedures of genetic engineering were performed by standard methods [23].

The promoter-probe plasmid pAA182 (about 11,000 bp) carrying the ampicillin resistance gene, pUC18 MCS and a promoterless *lac* operon [24] was kindly gifted by Professor S. Busby, (Birmingham, UK). The promoter activity of fragments cloned in multiple cloning sites (MCS) of this plasmid can be tested by changing of the phenotype of DH5α host cells from Lac$^-$ to Lac$^+$ on MacConkey agar plates [25].

The plasmid pLSR carrying the ampicillin resistance gene, an *Eco*RI-*Hin*dIII MCS of pUC18 and two identical divergently oriented bacteriophage λ oop transcription terminators was kindly gifted by Professor S. Busby (Birmingham, UK) [26].

5′-Phosphorylation of oligonucleotides using T4 polynucleotide kinase and ATP, as well as incorporation of 5′-^{32}P-label from γ-^{32}P-ATP, was carried out according to a published protocol [27].

DNA fragment "102d" (Fig. 1A) was stepwise assembled from synthetic oligonucleotides (see Supplementary material, Table S1) using T4 DNA ligase. At the first step 74-bp duplex ("74d") with 3′-protruding ends was obtained by enzymatic ligation of the oligonucleotides 17-cona1 + p25-cona2 + 22-cont2 + p20-cont + p32 with subsequent isolation on non-denaturing polyacrylamide gel. Upon 5′-phosphorylation the fragment "p74d" was ligated with oligonucleotide 28-pr. The resulting "102d" fragment was purified by electrophoresis.

2.1. Construction of plasmids

2.1.1. Plasmid pKDM-0

5′-Phosphorylated fragment "p102d" was ligated with *Sma*I-linearized and dephosphorylated pAA182 plasmid, and ligation mixture was used for transformation of DH5α strain. The ampicillin-resistant Lac+-transformants (red colonies) were selected on MacConkey agar plates with lactose. Clones with different orientations of the insert were selected by PCR analysis. The sequence of the plasmids in the region of insert was confirmed by DNA sequencing. The structure of the construct pKDM-0, containing the insert with selected orientation, is shown in Fig. 2B.

2.1.2. Plasmids pRLM-0 and pRLM1

To construct pRLM-0 plasmid the *Eco*RI-*Hin*dIII fragment of pKDM-0 was cloned into pRSL vector at *Eco*RI and *Hin*dIII sites.

The plasmid pRLM1 was prepared using high-efficient method of oligonucleotide-directed mutagenesis as described by Drutsa et al. [28]. Briefly, pRLM-0 plasmid was cut by *Hin*dIII restriction endonuclease and treated with exonuclease III to generate protruding single-stranded ends. Then the DNA prepared was annealed with 5′-phosphorylated mutagenic oligonucleotide p40-mhtr (for introduction of 16-bp insert with *Kpn*I site) and not phosphorylated oligonucleotide-adaptor 15-ahtl. The hybrid obtained was circularized with T4 DNA ligase, "filled in" with Klenow fragment of DNA polymerase, treated with T4 DNA ligase. Upon thermal inactivation of enzymes and extraction of the mixture with phenol/chloroform DNA was precipitated, re-dissolved, treated with DNA polymerase I (nick-translation) and used for transformation of the *E. coli* ER1821 cells. The sequence of 16-bp insert region was confirmed by DNA sequencing.

2.1.3. Auxiliary plasmids of pBH series

To facilitate the reconstruction of interpromoter region the *Eco*RI-*Hin*dIII-fragment of pRLM1 plasmid was sub-cloned in small laboratory pB1 vector (1707 bp, pUC19 origin of replication, ampicillin resistance gene, pUC19 MCS) lacking λ oop terminators. The resulting pBH1 plasmid (1839 bp) was used as a template for whole-plasmid PCR-mutagenesis [29] using primers p24-cont2 and p32-kib to introduce 11-bp insert in interpromoter region. The resulting pBH2 plasmid (1850 bp) was used to construct pBH3 plasmid (1865 bp). To this end pBH2 plasmid was cut by *Psp*OMI restriction endonuclease and ligated with two annealed oligonucleotides p15-xbup and 15-bxdo. At the next step the plasmid pBH3 was used for preparation of pBH4 plasmid (1891 bp). For this purpose, the unmethylated plasmid pBH3(met$^-$), isolated from *E. coli* JM110 carrying pBH3 plasmid, was cut by *Xba*I restriction endonuclease and ligated with two annealed oligonucleotides 26-up and 26-do.

The pBH2 plasmid was used as a starting point for preparation of two constructs with mutations in either leftward or rightward promoter, i.e. pBH2(L$^-$) and pBH2(R$^-$). In the first case, pBH2 plasmid was cleaved with restriction endonucleases *Eco*RI and *Psp*OMI, the ends were "filled in" with the Klenow enzyme, and DNA was recircularized by DNA ligase to generate plasmid pBHL containing single leftward promoter. To create pBHR plasmid with single rightward promoter, pBH2 plasmid was cleaved with restriction endonucleases *Hin*dIII and *Xho*I, the ends were "filled in" with the Klenow enzyme and DNA was recircularized. To generate plasmids pBHR(mut) and pBHL(mut) with identical substitutions in "−10" and "−35" promoter elements, the pBHR and pBHL plasmids were used as templates in two separate experiments on the whole-plasmid mutagenesis with the use of primers 16-pstt and 21-pptb. Then *Eco*RI-*Psp*OMI-fragment from pBHR(mut) was inserted between the *Eco*RI and *Psp*OMI sites of pBH2 plasmid to generate pBH2(R$^-$) plasmid, while *Xho*I-*Hin*dIII-fragment from pBHL(mut) was inserted

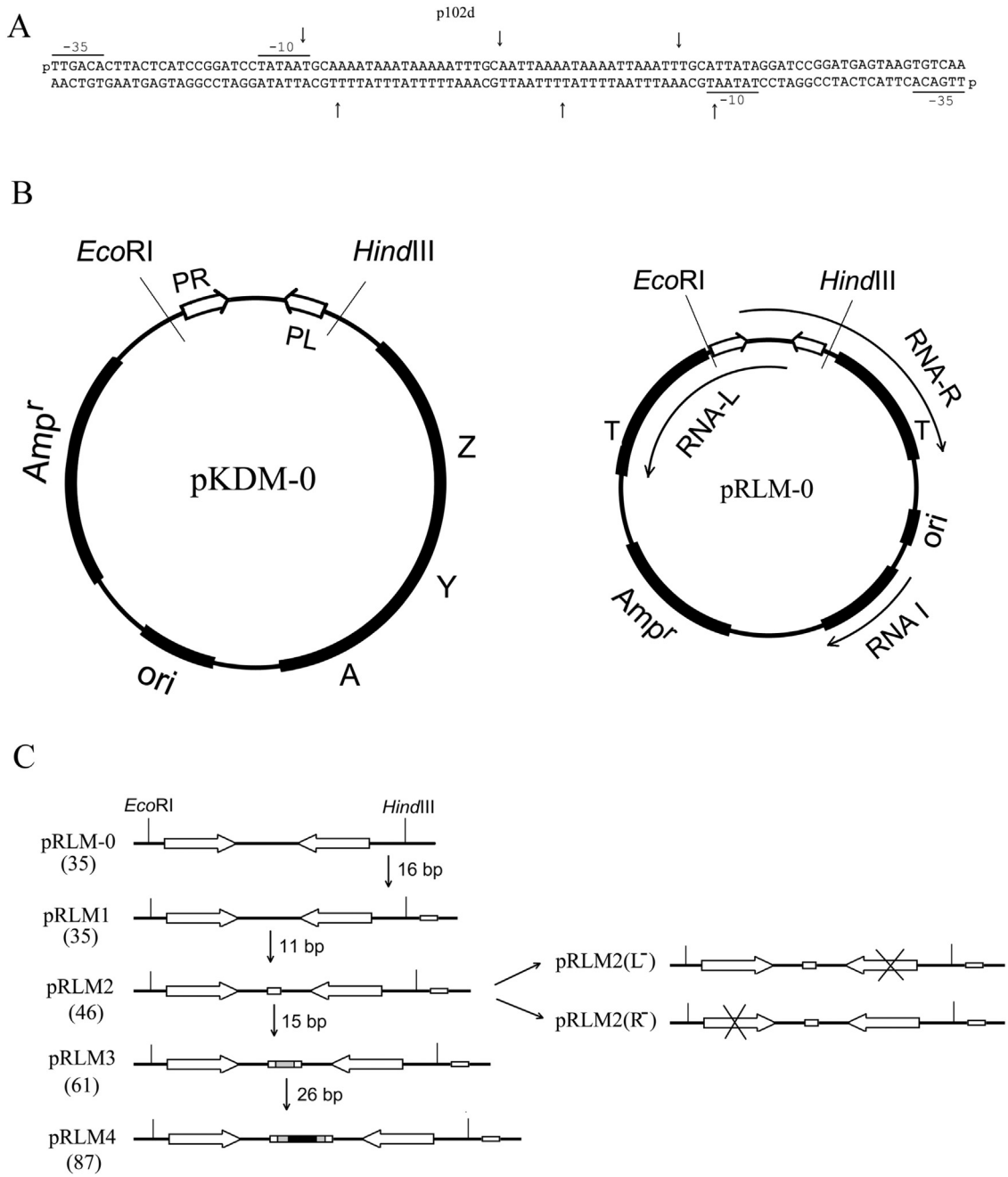

Fig. 1. DNA constructs used in this study. A. Nucleotide sequence of 102-bp synthetic fragment "p102" with convergently arranged identical 30-bp consensus promoter structures. Vertical arrows denote the junction between oligonucleotides used for the assembly of the duplex. "−10" and "−35" promoter elements are over- and underlined. B. Map of the basic plasmids pKDM-0 (left) and pRLM-0 (right) with convergent promoters. To prepare pKDM-0 fragment "p102" was cloned at *Sma*I site of pAA182 vector, which contains ampicillin resistance gene (Amp^r), genes of the promoterless *E. coli lac* operon (Z, Y and A) and the origin of replication (ori). To prepare pRLM-0 plasmid the *Eco*RI-*Hin*dIII-fragment of pKDM-0 was cloned in pLSR vector, which contains two divergently arranged identical bacteriophage λ oop terminators (T), replication origin (oriV) and gene for RNA I transcript (RNA I) [26]. Rightward and leftward promoters (PR and PL) in both plasmids are denoted by arrows. C. Scheme of the sequential reconstruction of the region of pRLM-0 plasmid, carrying two convergent promoters, to generate plasmids of pRLM series (for details see Materials and methods). The numbers in parentheses represent the distances between transcription start sites. Promoters, inactivated by mutagenesis, are crossed.

between *Xho*I and *Hin*dIII sites of pBH2 plasmid to generate pBH2(L^-) plasmid.

2.1.4. Plasmids of pRLM series

Plasmids pRLM2, pRLM3, pRLM4, pRLM2(R^-) and pRLM2(L^-) (Table 1 and Supplementary material, Fig. S1) were constructed by replacing the small *Eco*RI-*Hin*dIII-fragment in plasmid pRLM1 with the small *Eco*RI-*Hin*dIII-fragments from plasmids pBH2, pBH3, pBH4, pBH2(R^-) and pBH2(L^-), respectively. The correct sequence of the promoter regions in the resulting plasmids was confirmed by DNA sequencing.

2.2. Identification of transcription start sites

Transcription start sites in the region of convergent promoters of the plasmid pKDM-0 were determined by S1-nuclease mapping according to protocol [30]. RNA was extracted from DH5α cells carrying pKDM-0 plasmid. Two DNA probes, ^{32}P-labeled at only one strand, were obtained by PCR with primers ^{32}P-p25PAA plus 20KOR (or ^{32}P-p20KOR plus

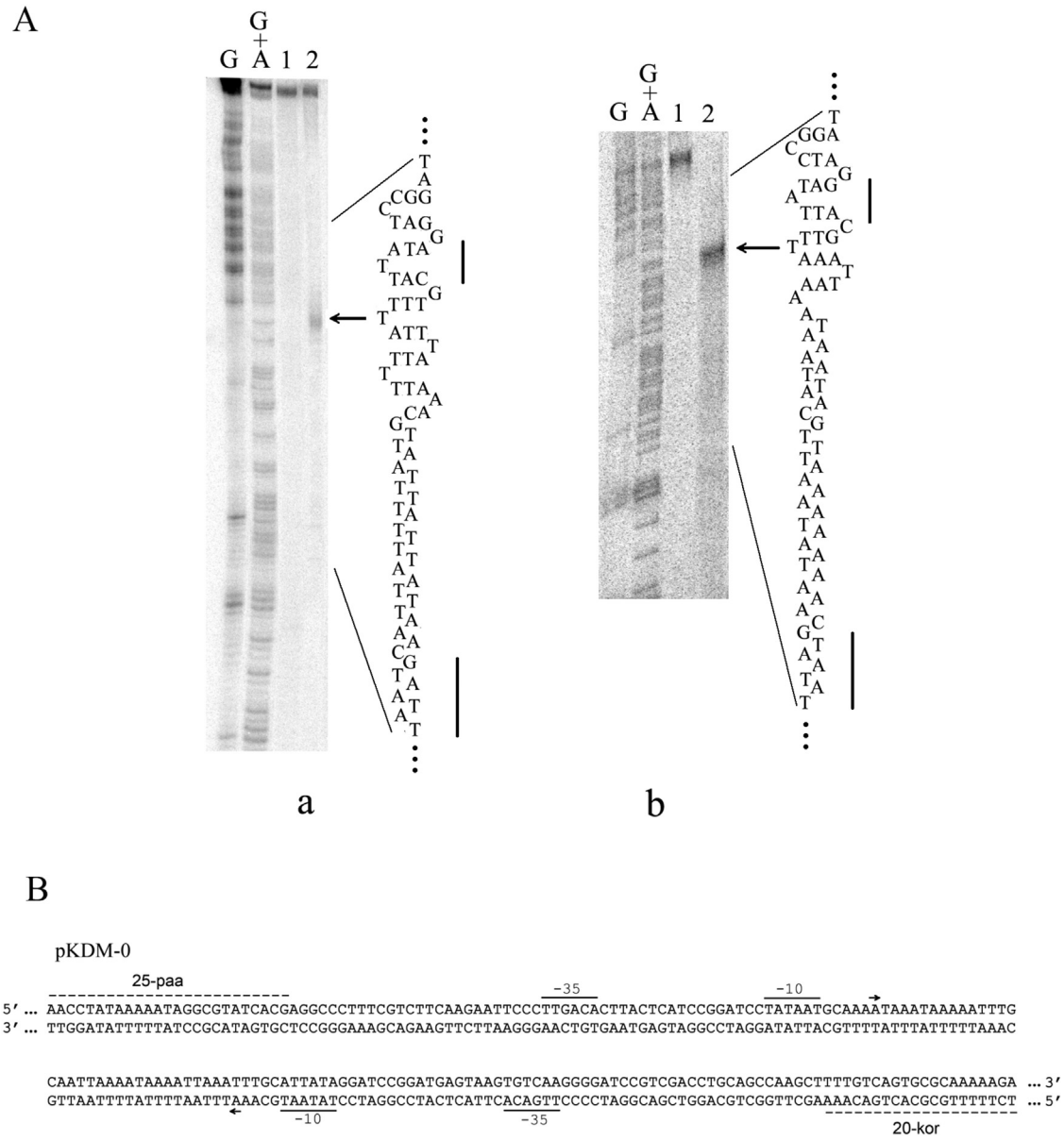

Fig. 2. Identification of transcription start sites. A. Mapping of the rightward (A, *a*) and leftward (A, *b*) transcription start sites in the region of convergent promoters of the pKDM-0 plasmid. Arrows point to the positions of ^{32}P-labeled fragments obtained by PCR with primers ^{32}P-p25-paa and 20-kor (a, column 2) or 25-paa and ^{32}P-p20-kor (b, column 2) and protected from S1 nuclease hydrolysis by hybridization with total RNA isolated from cells transformed with plasmid pKDM-0. Columns 1 correspond to untreated ^{32}P-labeled fragments. Columns "G" and "A + G" are the sequence ladders generated by chemical modification and cleavage of the same DNA fragments according to the Maxam-Gilbert protocol [41]. Vertical segments denote the position of "−10" promoter elements. B. Sequence of the promoter region of pKDM-0 plasmid. Arrows indicate the transcription start sites.

Table 1
Characteristics of the plasmids with convergent promoters constructed in the present work.

Name	Plasmid size, bp	Distance between tss[a], bp	Size of RNA-R[b], nt	Size of RNA-L[b], nt	Ratio[c] of transcripts RNA-R to RNA-L
pRLM0	2660	35	178	182	–
pRLM1	2676	35	194	182	2.4
pRLM2	2687	46	205	193	2.2
pRLM3	2702	61	220	208	1.4
pRLM4	2728	87	246	234	3.6
pRLM2(L$^-$)	2687	–	205	–	–
pRLM2(R$^-$)	2687	–	–	193	–

[a] tss - transcription start sites.
[b] RNA-R and RNA-L - the rightward and leftward transcripts, nt – nucleotide.
[c] Data obtained from the *in vitro* transcription experiments, presented in Fig. 3.

25PAA) and plasmid pKDM-0 as template. The probes were hybridized to RNA at 50 °C for 3 h, treated with S1 nuclease (200 units) for 1 h at 25 °C and applied on sequencing gel (Fig. 2A).

2.3. Single-round transcription

Experiments were carried out according to our published protocol [31]. Transcription was performed by incubation of plasmid DNA template (5–10 nM) with RNAP (30–50 nM) in transcription buffer (40 mM Tris-HCl pH 8.0, 10 mM $MgCl_2$, 100 mM KCl, 1 mM dithiothreitol, 5% glycerol, 100 μg/ml bovine serum albumin) for 5 min at 37 °C, followed by the simultaneous addition of ribonucleoside triphosphates (NTPs) and heparin to yield the following final concentrations: 100 μg/ml of heparin, 100 μM (each) NTPs (ATP, GTP, CTP) and 10 μM [^{32}P]UTP (specific activity of 50 cpm/fmol). The total reaction volume was 10 μl. Upon incubation for 10 min at 37 °C, the reaction was stopped

by adding 5 μl of stop solution (20 mM EDTA, 80% deionized formamide, 0.1% xylene cyanol, 0.1% bromophenol blue) and heating it to 75 °C for 30 s. Samples were analyzed by denaturing 8% gel electrophoresis and quantified using a Molecular Dynamics PhosphorImager and ImageQuant software.

2.4. Preparation of binary DNA-RNAP complexes for AFM studies

Plasmid DNA of pRLM series (1 nM) was incubated with RNAP (3–5 nM) in 10 μl of transcription buffer without BSA for 20 min at 37 °C and the reaction mixture upon dilution (100–1000 fold) was deposited on freshly cleaved mica and studied using AFM.

2.5. Atomic force microscopy

For AFM study, a 10 μl portion of plasmids or open promoter complexes (with DNA concentration 1 μg/ml) in the buffer (4 mM TrisHCl, 2 mM $MgCl_2$, 10 mM NaCl) was deposited onto freshly cleaved mica for 10 min. After that the sample was dried in air flow and washed by exposing its surface to a 100 μl droplet of distilled water for 1 h. Then, after drying in air flow, the samples were ready for AFM study.

AFM experiments were performed in air using multimode atomic force microscope Nanoscope 3a (Digital Instruments, USA). The AFM images were obtained in tapping mode using HA_NC cantilevers (NT-MDT, Russia) with a monocrystal silicon tip exhibiting a curvature radius of about 10 nm. The scan rate was typically 2.1 Hz with 512 × 512 pixels. The AFM scan size was typically about 500 × 500 nm to achieve high pixel resolution (~1 nm per pixel) to be able to discriminate single OPC from two closely located ones. Image processing was performed using the FemtoScan Online software (Advanced Technologies Center, Russia).

3. Results and discussion

3.1. Construction of the plasmids with convergent promoters

With the purpose to investigate the effects of the structural factors on TI in the context of convergent transcription, a special system was designed. It represents a set of plasmid constructions, containing a module with two face-to-face oriented identical artificial constitutive promoters, recognized by *E. coli* RNA polymerase. The constructs differ in the distance between promoters. The starting point for this work was synthetic 102 bp DNA fragment "p102d" and two promoter-probe plasmids pAA182 [25] and pLSR [26] (Fig. 1A,B). At the edges of "p102d" fragment there are two 30 bp inverted repeats of promoter-like structure with consensus "−10" (TATAAT) and "−35" (TTGACA) elements, separated by 17 bp spacer. It has been previously shown that insertion of such 30-bp synthetic duplex into the plasmid generates a sufficiently strong transcription initiation signal [32]. To characterize the in vivo functionalities of the two convergent promoters, the "p102d" fragment was cloned in pAA182 plasmid at the unique *Sma*I site upstream of promoterless *lac*-operon. Analysis of recombinant plasmids, isolated from the *E. coli* DH5α transformants, demonstrating $lacZ^+$ phenotype (red colonies on indicator MacConkey agar plates), has shown the presence of the 102 bp segment inserted in both orientations, indicating that, despite differences in the sequence of flanking regions both promoters are active in vivo. One of the constructs (pKDM-0) (Figs. 1B and 2B) was selected for further experiments.

The next step was the construction of the basic plasmid for the *in vitro* investigation of convergent transcription. The starting point for this was pLSR vector, carrying an *Eco*RI-*Hin*dIII polylinker and two identical divergently oriented bacteriophage λ *oop* transcription terminators [26]. (It should be noted, that there is also separately located RNA I promoter, directing synthesis of 107-mer transcript, which can be used as an internal control for quantification of the activity of bidirectional promoters). This vector has proved to be quite useful for study the divergent transcription [26]. The *Eco*RI-*Hin*dIII fragment from pKDM-0 plasmid with two convergent promoters was inserted between *Eco*RI and *Hin*dIII sites of pLSR. The resulting plasmid pRLM-0, when used as a template in transcription reactions, catalyzed by *E. coli* RNA polymerase, provides for different-sized transcripts, initiated from leftward (182 nucleotides) and rightward (178 nucleotides) promoters. Since these two transcripts are close in size, their resolution on polyacrylamide gel can be problematic. To overcome this problem, the pRLM-0 plasmid was reconstructed by inserting a 16-bp fragment downstream from *Hin*dIII site (yielding the plasmid pRLM1), which resulted in increase of the rightward transcript size up to 194 nucleotides (Table 1, Fig. 1C and Supplementary material, Fig. S1).

The next step of our work was the construction of a set of plasmids-homologs of pRLM1, which are characterized by stepwise increase in the distance between two convergent promoters (Fig. 1C, Table 1 and Supplementary material, Fig. S1).

Three sequential rounds of genetic engineering experiments on introduction of 11 bp, 15 bp and 26 bp fragments into the region between two promoters (using either whole-plasmid PCR mutagenesis or standard procedures of fragment fusion at restriction sites) yielded the plasmids pRLM2, pRLM3 and pRLM4 (Table 1, Fig. 1C and Supplementary material, Fig. S1). Two additional plasmids (pRLM2 analogs) with inactivated either rightward (pRLM2(R^-)) or leftward (pRLM2(L^-)) promoters were also constructed. The inactivation of promoters was achieved by multiple substitutions within −10 and −35 regions (Table 1, Fig. 1C and Supplementary material, Fig. S1).

3.2. Activity of convergent promoters

To confirm the in vivo activity of both promoters the construct pKDM-0 was used for identification of transcription start sites using S1-nuclease mapping technique. The results indicate the presence of two transcripts, initiated from both promoters in opposite directions (Fig. 2).

The suitability of the pLRM-plasmids as templates for *in vitro* TI investigation was demonstrated in a series of single-round transcription experiments carried out with *E. coli* RNA polymerase. Analysis of the reaction mixtures using polyacrylamide gel electrophoresis has shown the presence of RNAs, corresponding in their length to the transcripts, initiated from two convergent promoters (Fig. 3A). The relatively high intensity of the bands, corresponding to these transcripts, compared to that of RNA I, indicates that both promoters are very strong transcription initiation signals. The quantification of the transcripts allowed one to reveal some interesting features. First, there is some difference in the strength of two promoters with rightward promoter being about 1.5-fold stronger than leftward, as can be seen from the results of transcription of pRLM(R^-) and pRLM(L^-) plasmids (Table 1, Fig. 3B). The explanation may be as follows: although the "core" structures (30-bp fragments) of promoters are identical, the flanking regions are different and provisionally modulate the promoter strength. Besides, in case of face-to-face arranged promoters (constructs pRLM1–pRLM4) significant suppression of both of them was observed. It is noteworthy, that the degree of the suppression of weaker leftward promoter by rightward one is dependent on the interpromoter distance (Table 1). The molar ratio of transcripts (RNA-R/RNA-L) varied in the range of 1.4–3.6.

3.3. Characterization of plasmids and open promoter complexes using AFM

In most previous studies of the mechanisms of TI (realized with the use of both linear and circular supercoiled templates) the role of "higher-order" structure of DNA template has not been considered. However, we assume that transcriptional interference may be also influenced by the factors intrinsic to the circular templates such as superhelicity and connected with it additional bends and other structures. Therefore, our interest is to use circular DNA plasmids for investigation of transcription complexes. First of all, we have characterized

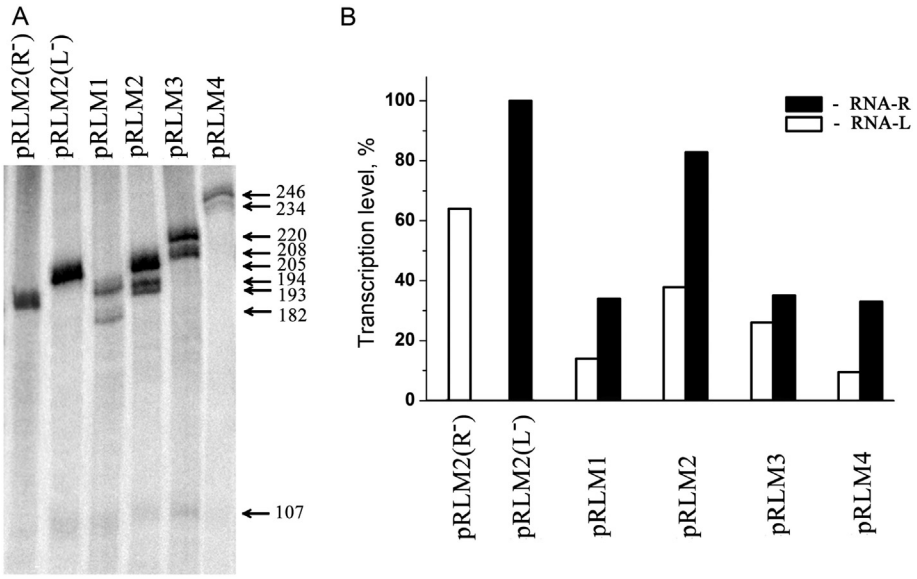

Fig. 3. *In vitro* transcription of the plasmids of pRLM series. A. Radioautograph of the electrophoretic separation in 8% denaturing polyacrylamide gel of the one-round transcription products, obtained from single promoter or two convergent promoters of pRLM plasmids. Arrows with numbers on the right indicate the positions and sizes of the transcripts. The 107-mer corresponds to RNA I transcript encoded by the vector and used as an internal control. B. The diagram of transcription level in experiments presented in the electrophoregram (panel A). The radioactive bands, corresponding to full-length transcripts (rightward (RNA-R) and leftward (RNA-L)) were quantitated, normalized to the quantity of internal control RNA I in each lane and to the U content of each transcript, and then presented as a percentage of the amount of transcript generated from promoter pRLM2(L^-). The experiments were repeated at least three times, and the standard deviation from the mean did not exceed 12% for each type of plasmid.

DNA plasmids of pRLM series using AFM. For this purpose, we have deposited freshly prepared DNA plasmids onto a mica surface using standard procedure (see Experimental section). Each of these DNA templates contains two convergently aligned promoters separated by different number of base pairs (from 35 to 87, see Table 1 and Supplementary material, Fig. S1). Typical AFM images of pRLM1–pRLM4 plasmids adsorbed on mica surface from the buffer solution (4 mM Tris-HCl, 2 mM $MgCl_2$, 10 mM NaCl) have demonstrated their closed contours (Fig. 4), as it was expected. Some DNA molecules have also formed hairpin structures (Fig. 4E-F), which is probably the consequence of superhelicity of these DNA plasmids. Their contour lengths estimated from AFM images, demonstrate correlation with the number of base pairs of these plasmids (Table 2, the number of the analyzed plasmid molecules N was 50 for each plasmid type).

Next, we have studied the formation of promoter-specific (open) complexes with DNA plasmids pRLM2, pRLM3 and pRLM4 using AFM. RNAP-DNA complexes were obtained by mixing of the corresponding DNA plasmids with RNAP holoenzyme in the transcription buffer using standard procedure (see Materials and methods). AFM images of the resulting samples deposited on mica have revealed the presence of circular DNA structures like those shown in Fig. 4; some of these plasmids contained one or two closely spaced globules 3–4 nm in height, which we interpreted as DNA bound RNA polymerases (Figs. 5 and 6). Since the formation of an OPC is accompanied by significant bending of the promoter DNA axis [33–35], we have attributed the observed single RNAP-DNA complexes to OPCs if they demonstrated the characteristic DNA bend at an RNAP binding site. The observation frequency of OPCs was ~25% independent of the plasmid (the number of the analyzed plasmid molecules N was about 100 for each plasmid type). Typical AFM images of single OPCs are presented in Fig. 5 for each studied plasmid (pRLM2, pRLM3 and pRLM4). The observed DNA bends are zoomed in the right column of Fig. 5.

Two closely located DNA bound RNAPs were referred to as convergent OPCs. Such complexes were revealed for each of the three plasmids (pRLM2, pRLM3 and pRLM4, Fig. 6); however, their structure and observation frequency were different.

Remarkably, two RNAPs bound to the pRLM2 and pRLM4 DNA templates line up along the apparent DNA contour (Fig. 6A,I), while the enzyme molecules bound to the pRLM3 plasmid line up across the contour of a DNA template (Fig. 6B–H). This difference can be explained by the already mentioned fact that RNAP bends DNA in the promoter region upon OPC formation [34], which is schematically shown in Fig. 7A. The combination of the DNA bends in the regions of two closely located OPCs results in two different outcomes (Fig. 7B,C), which are similar to those observed in Fig. 6: two RNA polymerases arrange along a DNA contour (and from one side of the DNA template, Fig. 7B) or across it (and from different sides of the DNA template, Fig. 7C). Variability of the "out-of-contour" orientations of double complexes observed on pRLM3 DNA template (Fig. 6B–H) may be connected with the DNA flexibility and its reorientation on the surface during relaxation.

Analysis of a large number of AFM images of pRLM2 and pRLM4 templates incubated with RNAPs indicates that the formation of two closely spaced OPCs on this template is a very rare event for both of these plasmids. Indeed, we have found one such complex for each of these two plasmids after examination of more than one hundred templates (observation frequency q ~ 1%, N ~ 100). At the same time, the observation frequency of double OPCs for pRLM3 plasmid was ~20% (N ~ 100) that is at least 20 times higher. Presumably, the formation of double complexes is hindered on pRLM2 and pRLM4 template by the steric confinement, connected with the configuration of DNA bends, which form a pocket-like structure (Fig. 7B). In contrast, different spatial arrangement of convergent promoters of pRLM3 plasmid leads to another orientation of double complexes without formation of a pocket-like structure. Therefore, in the latter case the formation of double OPCs is much more favorable.

3.4. Model of the TI

In this work, basing on the obtained results and literature data, we propose the model of transcription interference for convergent promoters. As it was already mentioned, DNA experiences a bend upon binding with RNAP [36,37]. This bend is often observed in AFM images of OPCs [38,39] (Fig. 5). RNAP binds with DNA asymmetrically to its axis: the most part of the enzyme is located from one side of DNA double helix [37]. Moreover, there is evidence that DNA may wrap around

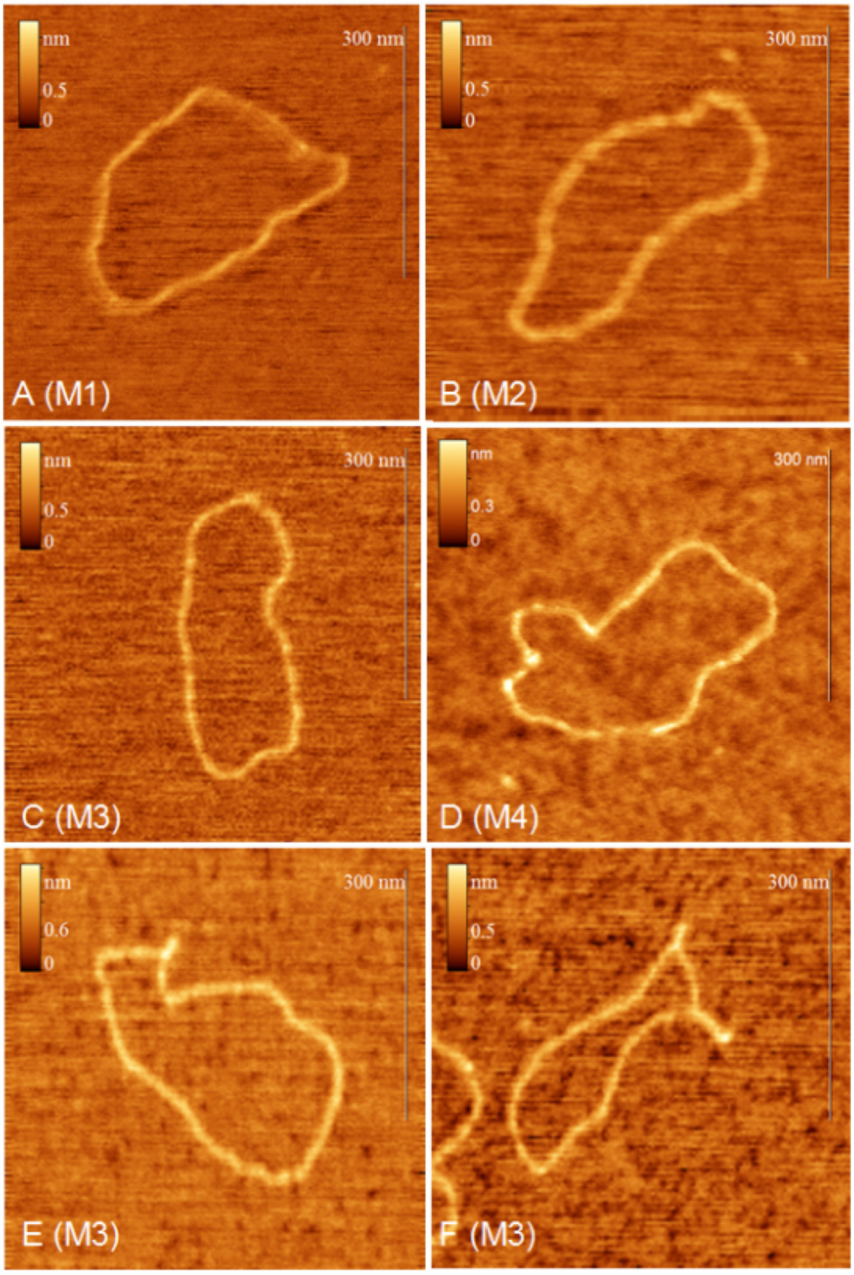

Fig. 4. Montage of AFM images of plasmids pRLM1–pRLM4 (M1–M4). Image size is 500 × 500 nm.

RNAP [18,19,36,38]. It should be mentioned, that the extent of bending and even wrapping of DNA around RNAP is dependent on the structure of promoters [34]. It has been shown that DNA wrapping around RNAP in open promoter complexes is dependent on the contacts of enzyme with A/T-rich UP elements located upstream of the −35 hexamer [38, 39]. Since the plasmids used in our work do not contain pronounced UP elements (Fig. S1), we do not expect DNA wrapping around RNAP in our open promoter complexes. However, the proposed model of formation of closely spaced open promoter complexes may be extended for the case with DNA wrapping (Supplementary material, Fig. S2).

Table 2
AFM measured contour length of plasmids pRLM1–pRLM4 in nm and b.p. (assuming DNA B-form).

Plasmid name	Length, b.p.	Contour length, nm (b.p.)	Standard deviation, nm (b.p.)
pRLM1	2676	883 (2597)	28 (82)
pRLM2	2687	914 (2688)	32 (94)
pRLM3	2702	915 (2691)	45 (132)
pRLM4	2728	942 (2771)	42 (124)

In the case of closely spaced promoters (when the spacing is comparable to RNAP size) two OPCs may experience steric constraints from each other, and small variation in the number of nucleotides between two promoters results not only in the change of the distance between complexes but also in their turn around DNA scaffold. In two extreme events the complexes may be located either from the same side of DNA double helix or from its opposite sides, i.e., two different local DNA configurations will be observed: U-like (*cis*-configuration) or S-like (*trans*-configuration) (Fig. 7B–C). Moreover, there are many intermediate alternatives of mutual locations of transcription complexes corresponding to their different rotation with regard to each other. So, the configuration of two transcription complexes on DNA is defined by the interpromoter distance, which determines the rotation of the promoters and, therefore, RNAP molecules around each other.

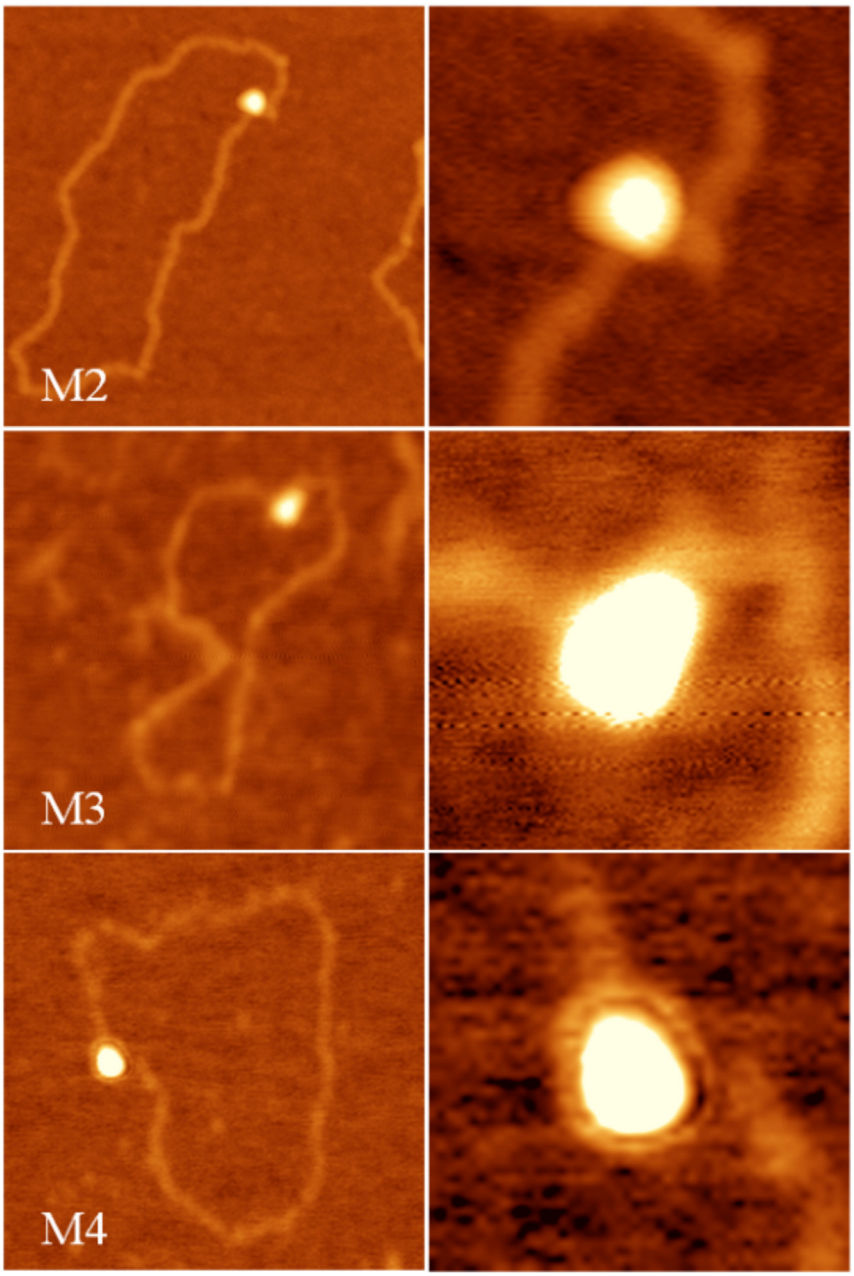

Fig. 5. Montage of AFM images of single open promoter complexes with plasmids pRLM2 (M2), pRLM3 (M3) and pRLM4 (M4) (left) and zoomed areas around RNAP (right). Image size is 375 × 375 nm (left) and 100 × 100 nm (right).

Moreover, for supercoiled circular DNA these local configurations may be fixed to a larger extent than for linear DNA scaffolds due to the fact that circular DNA has less degree of freedom. With the increase of the interpromoter distance the identical configurations of complexes in three dimensions will be repeated with the interval equal to a multiple of DNA helical turns. It is obvious, that in case of *cis*-configuration two RNAPs are more capable to interfere, and RNAP molecule bound to the stronger promoter (with formation of an OPC) may prevent the formation of an OPC by the second enzyme on the near-by promoter because of the failure to accommodate two RNAP molecules in the "narrow pocket".

This explains the previously reported effect of suppression of a "weak" promoter by a stronger one [4,5,7] as well as the effects observed in our system. This model of TI is an alternative to other known mechanisms of interference (e.g., the model of «sitting ducks») implying the direct contact (collision) of two RNAPs moving along the DNA. Our model supposes distant interaction of RNAPs via the change of local configuration of DNA connected with its bending. The results obtained in this work support this model of TI. The region of the convergent promoters in the constructed plasmids is characterized by the following parameters: the distance between the transcription start sites in the original construction pRLM1 is 35 bp that corresponds to 3.3 turns of DNA double helix (assuming 10.5 bp per one turn). The distance between the transcription start sites in the plasmids pRLM2, pRLM3 and pRLM4 successively increases (regarding to pRLM1 structure) by the following number of turns: 1, 2.5 and 5 accordingly. Therefore, the mutual configuration of transcription start sites in three dimensions for pRLM1, pRLM2 and pRLM4 (for which the distances between these sites differ by integral numbers of helical turns) and consequently the architecture of RNAP-DNA complexes would be similar. As for pRLM3 plasmid, the spatial arrangement of two RNAP molecules will be opposite, since the distance between transcription start sites differs

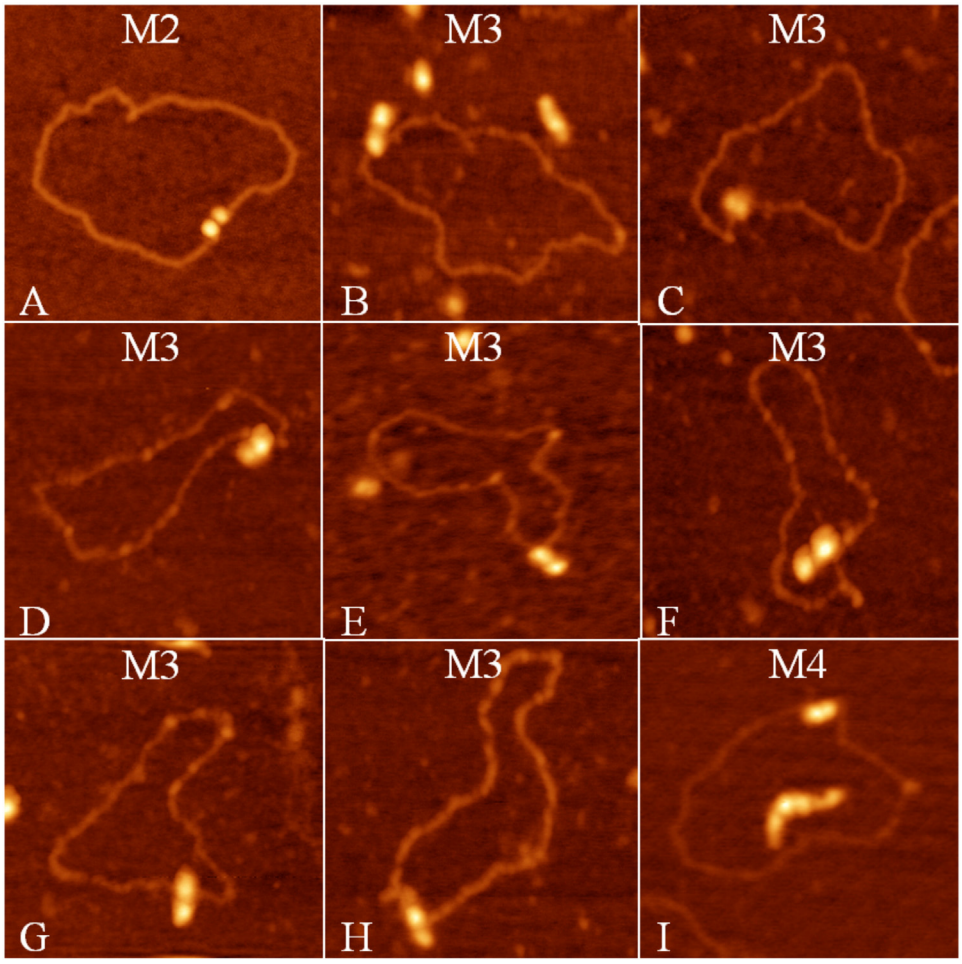

Fig. 6. Montage of AFM images of double open promoter complexes with plasmids pRLM2 (M2), pRLM3 (M3) and pRLM4 (M4). Image size is 400 × 400 nm.

from that of the other pRLM constructs by integral numbers of turns plus a half-turn.

Indeed, our AFM studies and transcription assays have demonstrated that properties of pRLM3 plasmid were different from those of other DNA constructs. In particular, the transcripts ratio RNA-R/RNA-L has demonstrated the minimal value of 1.4 for pRLM3 plasmid (which is close to the activity ratio of individual promoters), whereas for other DNA constructs this value is higher, being in the range of 2.2–3.6 (Table 1). Besides, the constructs exhibit differences in the reduction of the overall transcription levels. These findings definitely testify in favor of mutual interplay between two transcriptional units and suggest the importance of DNA conformation in TI. According to the published footprinting data on the OPCs, the downstream border of the DNA region covered by RNA polymerase lies near +20 position [40]. Then, the linear distance between convergent promoters (at least for the constructs pRLM2-M4) is enough for accommodation of two RNAP molecules. If spatial factors did not contribute to TI, the patterns of transcription would be identical in all cases. Apparently, two OPCs form on pRLM3 plasmid S-like structure (*trans*-configuration, Fig. 7C,E), where two RNAP molecules may simultaneously bind

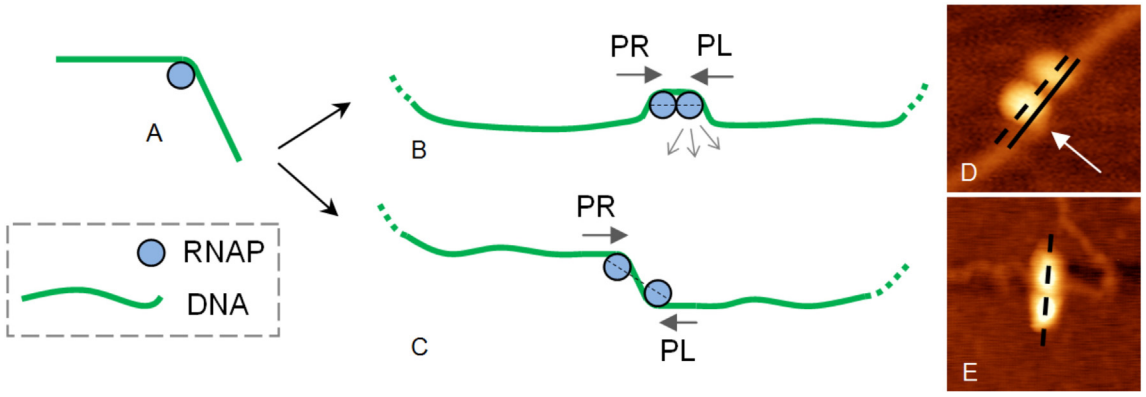

Fig. 7. Schematic representation of (A) single open promoter complex, (B–C) two possible configurations of two closely located open promoter complexes interpreting the observed AFM images. (D–E) Zoomed (from Fig. 6) AFM images of two closely located open promoter complexes, illustrating cases (B) and (C). White arrow in (D) indicates a DNA bend near RNAP molecule. Dotted lines connect the centers of RNAP molecules. Solid line shows a DNA contour in the area of OPCs on the assumption of absence of DNA bending.

promoters without hindering each other. In contrast, convergent OPCs tend to form *cis*-configuration on pRLM1, pRLM2 and pRLM4 scaffolds, where protein molecules sterically hinder each other during the process of formation of an OPC ("narrow pocket", Fig. 7B,D). It should be noted, that for the systems of convergent promoters under study the contribution of other known mechanisms of TI (i.e. SD, collision, etc.) cannot be excluded. In particular, the reduced level of both transcripts in case of pRLM3 construct (both for R and L orientations) is apparently associated with additional interference caused by collision between two elongating RNAP molecules. In case of pRLM2 and pRLM4 the role of this factor in total TI seems to be less pronounced.

Our AFM results correlate well with transcription assays data: first, the proportion of double OPCs observed in AFM images is highest for pRLM3 plasmid, indicating the most favorable configuration for simultaneous formation of two OPCs. Moreover, the morphology of double OPCs with pRLM3 plasmid differs from the morphology of those with pRLM2 and pRLM4 plasmids. In the first case two close DNA bends form "S-like" structure as shown in Fig. 7C (depending on the bending angle of DNA at the point of its binding with RNAP, the resulting "S-like" structure may look slightly different). Though we cannot follow a DNA contour in close proximity of OPCs in AFM images due to protein broadening by an AFM tip, the mutual configuration of two proteins relatively to the apparent DNA contour supports the model of "S-like" configuration: two protein molecules are located "across" the apparent DNA contour (Fig. 7E). In the case of pRLM2 and pRLM4 plasmid, AFM images sometimes resolve a DNA bend at double OPCs (e.g., see the arrow in Fig. 7D). Another argument, which supports the presence of the DNA kink in this case, is the position of two RNAP molecules relatively to the apparent DNA thread. A solid line in the AFM image in Fig. 7D (which is an enlarged region of Fig. 6A) shows a DNA contour in the area of OPCs on the assumption of absence of DNA bending. We can see that neither of protein molecules is located on the solid line, suggesting that DNA is severely bent in this region. The observation that both RNAP molecules are located from the same side of the dotted line and parallel to it (compare the dotted line connecting RNAP centers with the solid line) highlights the pocket-like configuration (Fig. 7B).

The proposed model demonstrates in a simplified way the appearance of what we call "narrow pocket" mechanism. The main reason of the appearance of this effect is DNA bending, induced by RNAP interaction with promoters. The mutual orientation of two bends is dependent on the interpromoter spacing and ultimately defines productive transcriptional output.

4. Conclusion

With the purpose to investigate the mechanisms of transcriptional interference, a series of new plasmids with two convergent promoters was constructed. The properties of these constructs were studied in the systems with RNA polymerase using AFM technique and *in vitro* run-off transcription assays. The effects observed allowed us to put forward a novel mechanism of transcription interference, which envisages the conformational transitions in DNA helix, associated with DNA bending upon binding of RNA polymerase with promoters.

Transparency document

The Transparency document associated with this article can be found, in online version.

Acknowledgements

This work was supported by Russian Foundation for Basic Research (grants 15-32-20629 and 13-04-01504).

Appendix A. Supplementary data

Supplementary data to this article can be found online at http://dx.doi.org/10.1016/j.bbagen.2016.06.026.

References

[1] A.C. Palmer, J.B. Egan, K.E. Shearwin, Transcriptional interference by RNA polymerase pausing and dislodgement of transcription factors, Transcription 2 (2011) 9–14, http://dx.doi.org/10.4161/trns.2.1.13511.
[2] K.E. Shearwin, B.P. Callen, J.B. Egan, Transcriptional interference – a crash course, Trends Genet. 21 (2005) 339–345, http://dx.doi.org/10.1016/j.tig.2005.04.009.
[3] K. Sneppen, I.B. Dodd, K.E. Shearwin, A.C. Palmer, R.A. Schubert, B.P. Callen, et al., A mathematical model for transcriptional interference by RNA polymerase traffic in *Escherichia coli*, J. Mol. Biol. 346 (2005) 399–409, http://dx.doi.org/10.1016/j.jmb.2004.11.075.
[4] H. Horowitz, T. Platt, Regulation of transcription from tandem and convergent promoters, Nucleic Acids Res. 10 (1982) 5447–5465, http://dx.doi.org/10.1093/nar/10.18.5447.
[5] D.F. Ward, N.E. Murray, Convergent transcription in bacteriophage λ: interference with gene expression, J. Mol. Biol. 133 (1979) 249–266, http://dx.doi.org/10.1016/0022-2836(79)90533-3.
[6] S. Adhya, M. Gottesman, Promoter occlusion: transcription through a promoter may inhibit its activity, Cell 29 (1982) 939–944, http://dx.doi.org/10.1016/0092-8674(82)90456-1.
[7] B.P. Callen, K.E. Shearwin, J.B. Egan, Transcriptional interference between convergent promoters caused by elongation over the promoter, Mol. Cell 14 (2004) 647–656, http://dx.doi.org/10.1016/j.molcel.2004.05.010.
[8] M. Nagornykh, M. Zakharova, A. Protsenko, E. Bogdanova, A.S. Solonin, K. Severinov, Regulation of gene expression in restriction-modification system Eco29kI, Nucleic Acids Res. 39 (2011) 4653–4663, http://dx.doi.org/10.1093/nar/gkr055.
[9] A.C. Palmer, A. Ahlgren-Berg, J.B. Egan, I.B. Dodd, K.E. Shearwin, Potent transcriptional interference by pausing of RNA polymerases over a downstream promoter, Mol. Cell 34 (2009) 545–555, http://dx.doi.org/10.1016/j.molcel.2009.04.018.
[10] S.K. Eszterhas, E.E. Bouhassira, D.I.K. Martin, S. Fiering, Transcriptional interference by independently regulated genes occurs in any relative arrangement of the genes and is influenced by chromosomal integration position, Mol. Cell. Biol. 22 (2002) 469–479, http://dx.doi.org/10.1128/MCB.22.2.469-479.2002.
[11] O.E. Andrews, D.J. Cha, C. Wei, J.G. Patton, RNAi-mediated gene silencing in zebrafish triggered by convergent transcription, Sci. Rep. 4 (2014), http://dx.doi.org/10.1038/srep05222.
[12] M. Gullerova, N.J. Proudfoot, Convergent transcription induces transcriptional gene silencing in fission yeast and mammalian cells, Nat. Struct. Mol. Biol. 19 (2012) 1193–1201, http://dx.doi.org/10.1038/nsmb.2392.
[13] J. Georg, W.R. Hess, *cis*-Antisense RNA, another level of Gene regulation in bacteria, Microbiol. Mol. Biol. Rev. 75 (2011) 286–300, http://dx.doi.org/10.1128/MMBR.00032-10.
[14] A. Chatterjee, C.M. Johnson, C.-C. Shu, Y.N. Kaznessis, D. Ramkrishna, G.M. Dunny, et al., Convergent transcription confers a bistable switch in *Enterococcus faecalis* conjugation, PNAS 108 (2011) 9721–9726, http://dx.doi.org/10.1073/pnas.1101569108.
[15] N. Crampton, W.A. Bonass, J. Kirkham, C. Rivetti, N.H. Thomson, Collision events between RNA polymerases in convergent transcription studied by atomic force microscopy, Nucleic Acids Res. 34 (2006) 5416–5425, http://dx.doi.org/10.1093/nar/gkl668.
[16] C.W. Gibson, N.H. Thomson, W.R. Abrams, J. Kirkham, Nested genes: biological implications and use of AFM for analysis, Gene 350 (2005) 15–23, http://dx.doi.org/10.1016/j.gene.2004.12.045.
[17] D.J. Billingsley, W.A. Bonass, N. Crampton, J. Kirkham, N.H. Thomson, Single-molecule studies of DNA transcription using atomic force microscopy, Phys. Biol. 9 (2012) 021001, http://dx.doi.org/10.1088/1478-3975/9/2/021001.
[18] D.J. Billingsley, N. Crampton, J. Kirkham, N.H. Thomson, W.A. Bonass, Single-stranded loops as end-label polarity markers for double-stranded linear DNA templates in atomic force microscopy, Nucleic Acids Res. 40 (2012) e99, http://dx.doi.org/10.1093/nar/gks276.
[19] V. Gerganova, S. Maurer, L. Stoliar, A. Japaridze, G. Dietler, W. Nasser, et al., Upstream binding of idling RNA polymerase modulates transcription initiation from a nearby promoter, J. Biol. Chem. 290 (2015) 8095–8109, http://dx.doi.org/10.1074/jbc.M114.628131.
[20] Z. Sun, H.Y. Tan, P.R. Bianco, Y.L. Lyubchenko, Remodeling of RecG helicase at the DNA replication fork by SSB protein, Sci. Rep. 5 (2015) 9625, http://dx.doi.org/10.1038/srep09625.
[21] C.N. Buechner, I. Tessmer, DNA substrate preparation for atomic force microscopy studies of protein-DNA interactions, J. Mol. Recognit. 26 (2013) 605–617, http://dx.doi.org/10.1002/jmr.2311.
[22] E.V. Dubrovin, S. Speller, I.V. Yaminsky, Statistical analysis of molecular nanotemplate driven DNA adsorption on graphite, Langmuir 30 (2014) 15423–15432, http://dx.doi.org/10.1021/la5041773.
[23] J. Sambrook, E.F. Fritsch, T. Maniatis, Molecular Cloning: A Laboratory Manual, second ed. Cold Spring Harbor Laboratory Press, New York, 1989.
[24] P.S. Jayaraman, T.C. Peakman, S.J.W. Busby, R.V. Quincey, J.A. Cole, Location and sequence of the promoter of the gene for the NADH-dependent nitrite reductase of *Escherichia coli* and its regulation by oxygen, the Fnr protein and nitrite, J. Mol. Biol. 196 (1987) 781–788, http://dx.doi.org/10.1016/0022-2836(87)90404-9.

[25] M. Casadaban, S. Cohen, Analysis of gene-control signals by DNA-fusion and cloning in *Escherichia coli*, J. Mol. Biol. 138 (1980) 179–207, http://dx.doi.org/10.1016/0022-2836(80)90283-1.
[26] M.S. El-Robh, S.J.W. Busby, The *Escherichia coli* cAMP receptor protein bound at a single target can activate transcription initiation at divergent promoters: a systematic study that exploits new promoter probe plasmids, Biochem. J. 368 (2002) 835–843, http://dx.doi.org/10.1042/bj20021003.
[27] O.N. Koroleva, V.L. Drutsa, N.G. Dolinnaia, A.V. Tsytovich, Z.A. Shabarova, DNA-like duplexes containing repetitive sequences. VII. Chemico-enzymatic synthesis of polymers with fragments of natural promotors, Mol. Biol. 18 (1984) 146–160.
[28] V. Drutsa, V. Kaberdin, Use of oligonucleotides and nick translation for site-directed mutagenesis in plasmids, Nucleic Acids Res. 20 (1992) 922, http://dx.doi.org/10.1093/nar/20.4.922.
[29] A. Hemsley, N. Arnheim, M. Toney, G. Cortopassi, D. Galas, A simple method for site-directed mutagenesis using the polymerase chain-reaction, Nucleic Acids Res. 17 (1989) 6545–6551, http://dx.doi.org/10.1093/nar/17.16.6545.
[30] H. Aiba, S. Adhya, B. Decrombrugghe, Evidence for 2 functional gal promoters in intact *Escherichia coli* cells, J. Biol. Chem. 256 (1981) 1905–1910.
[31] O.N. Koroleva, S.J.W. Busby, V.L. Drutsa, Effects of substitutions at position 180 in the *Escherichia coli* RNA polymerase sigma(70) subunit, J. Biosci. 36 (2011) 43–54, http://dx.doi.org/10.1007/s12038-011-9007-3.
[32] O. Koroleva, I. Shilov, V. Sergeev, V. Drutsa, Synthetic prokaryotic promoter .3. Cloning and *in vivo* functional activity, Mol. Biol. 28 (1994) 757–762.
[33] G. Kuhnke, H. Fritz, R. Ehring, Unusual properties of promoter-up mutations in the *Escherichia coli* galactose operon and evidence suggesting RNA polymerase-induced DNA bending, EMBO J. 6 (1987) 507–513.
[34] E.F. Ruff, M.T. Record, I. Artsimovitch, Initial events in bacterial transcription initiation, Biomolecules 5 (2015) 1035–1062, http://dx.doi.org/10.3390/biom5021035.
[35] Y. Zuo, T.A. Steitz, Crystal structures of the *E. coli* transcription initiation complexes with a complete bubble, Mol. Cell 58 (2015) 534–540, http://dx.doi.org/10.1016/j.molcel.2015.03.010.
[36] C. Rivetti, M. Guthold, C. Bustamante, Wrapping of DNA around the *E. coli* RNA polymerase open promoter complex, EMBO J. 18 (1999) 4464–4475, http://dx.doi.org/10.1093/emboj/18.16.4464.
[37] L. Mangiarotti, S. Cellai, W. Ross, C. Bustamante, C. Rivetti, Sequence-dependent upstream DNA-RNA polymerase interactions in the open complex with lambda P-R and lambda P-RM promoters and implications for the mechanism of promoter interference, J. Mol. Biol. 385 (2009) 748–760, http://dx.doi.org/10.1016/j.jmb.2008.11.019.
[38] N. Doniselli, P. Rodriguez-Aliaga, D. Amidani, J.A. Bardales, C. Bustamante, D.G. Guerra, et al., New insights into the regulatory mechanisms of ppGpp and DksA on *Escherichia coli* RNA polymerase-promoter complex, Nucleic Acids Res. 43 (2015) 5249–5262, http://dx.doi.org/10.1093/nar/gkv391.
[39] S. Cellai, L. Mangiarotti, N. Vannini, N. Naryshkin, E. Kortkhonjia, R.H. Ebright, C. Rivetti, Upstream promoter sequences and αCTD mediate stable DNA wrapping within the RNA polymerase–promoter open complex, EMBO Rep. 8 (2007) 271–278, http://dx.doi.org/10.1038/sj.embor.7400888.
[40] O. Ozoline, M. Tsyganov, Structure of open promoter complexes with *Escherichia coli* RNA-polymerase as revealed by the DNase-I footprinting technique - compilation analysis, Nucleic Acids Res. 23 (1995) 4533–4541, http://dx.doi.org/10.1093/nar/23.22.4533.
[41] A.M. Maxam, W. Gilbert, Sequencing end-labeled DNA with base-specific chemical cleavages, Methods Enzymol. 65 (1980) 499–560.